



UNIVERSITY OF LEEDS

This is a repository copy of *Eolian stratigraphic record of environmental change through geological time*.

White Rose Research Online URL for this paper:
<https://eprints.whiterose.ac.uk/180754/>

Version: Accepted Version

Article:

Cosgrove, GIE, Colombera, L orcid.org/0000-0001-9116-1800 and Mountney, NP orcid.org/0000-0002-8356-9889 (2021) Eolian stratigraphic record of environmental change through geological time. *Geology* (Boulder). ISSN 0091-7613

<https://doi.org/10.1130/G49474.1>

This is protected by copyright, all rights reserved. This is an author produced version of an article published in *Geology*. Uploaded in accordance with the publisher's self-archiving policy.

Reuse

Items deposited in White Rose Research Online are protected by copyright, with all rights reserved unless indicated otherwise. They may be downloaded and/or printed for private study, or other acts as permitted by national copyright laws. The publisher or other rights holders may allow further reproduction and re-use of the full text version. This is indicated by the licence information on the White Rose Research Online record for the item.

Takedown

If you consider content in White Rose Research Online to be in breach of UK law, please notify us by emailing eprints@whiterose.ac.uk including the URL of the record and the reason for the withdrawal request.



eprints@whiterose.ac.uk
<https://eprints.whiterose.ac.uk/>

1 Eolian Stratigraphic Record of Environmental Change 2 Through Geological Time

3 **G.I.E. Cosgrove¹, L. Colombera¹, N.P. Mountney¹**

4 ¹School of Earth and Environment, Institute of Applied Geophysics, University of Leeds, Woodhouse,
5 Leeds, LS2 9JT

6 **ABSTRACT**

7 The terrestrial sedimentary record provides a valuable archive of how ancient depositional systems
8 respond to and record changes in the Earth's atmosphere, biosphere and geosphere. However, the
9 record of these environmental changes in eolian sedimentary successions is poorly constrained and
10 largely unquantified. This study presents the first global-scale, quantitative investigation of the
11 architecture of eolian systems through geological time via analysis of 55 case studies of eolian
12 successions. Eolian deposits accumulating 1) under greenhouse conditions, 2) in the presence of
13 vascular plants and grasses, and 3) in rapidly subsiding basins, associated with the rifting of
14 supercontinents, are represented by significantly thicker eolian dune-set, sandsheet and interdune
15 architectural elements. Pre-vegetation eolian systems are also associated with more frequent
16 interactions with non-eolian environments. The interplay of these forcings has resulted in dune-set
17 thicknesses that tend to be smallest and largest in Proterozoic and Mesozoic successions, respectively.
18 In the Proterozoic, the absence of sediment-binding plant roots rendered eolian deposits susceptible to
19 post-depositional wind deflation and reworking by fluvial systems, whereby highly mobile channels
20 reworked contiguous eolian deposits. During the Mesozoic, humid greenhouse conditions (associated
21 with relatively elevated water-tables) and high rates of basin subsidence (associated with the break-up
22 of Pangea) favored the rapid transfer of eolian sediment beneath the erosional baseline. The common
23 presence of vegetation promoted accumulation of stabilizing eolian systems. These factors acted to
24 limit post-depositional reworking. Eolian sedimentary deposits record a fingerprint of major

25 environmental changes in Earth history: climate, continental configuration, tectonics, and land-plant
26 evolution.

27 **INTRODUCTION**

28 Eolian sedimentary systems are sensitive to environmental forcings, notably climate (Clemmensen et
29 al., 1994; Cosgrove et al., 2021a), tectonic configuration (Blakey et al., 1988), basin subsidence
30 (Kocurek and Havholm, 1993; Howell and Mountney, 1997; Cosgrove et al., 2021c), and the presence
31 and type of vegetation (Gibling and Davies, 2012; Santos et al., 2017, 2019). The preserved eolian
32 sedimentary record archives the response of eolian systems to changing environmental forcings
33 through geological time. However, despite a global sedimentary record, comparisons between eolian
34 systems developed under different environmental conditions are not straightforward: many
35 depositional models are qualitative and commonly derived from individual case studies (e.g. Kocurek
36 and Dott, 1981; Mountney and Jagger, 2004; Rodríguez-López et al., 2014).

37 Here, we undertake the first comprehensive comparison of the preserved architectures of eolian
38 systems accumulated and preserved through geological time. We consider 1) the thickness of eolian
39 architectural elements, 2) the relative proportion of different types of eolian elements, and 3) the
40 relationships of eolian strata with contiguous non-eolian deposits. The aim is to quantify variations in
41 eolian architectures at multiple scales of observation through geological time, and to interpret these
42 changes in terms of potential controls. Specific research objectives are 1) to determine which
43 environmental forcings markedly influence eolian architecture, and 2) to determine how these
44 forcings have acted and interacted through geological time.

45 **DATA AND METHODS**

46 This study utilizes the Database of Aeolian Sedimentary Architecture (DASA; Cosgrove et al., 2021a,
47 b, & c), which stores data on eolian and interdigitated non-eolian geological entities. Data considered
48 here are collated from 58 published accounts associated with 55 eolian successions. A location map of
49 all case studies and an account of the source literature is provided in Supplementary Information 1

50 and 2, respectively. Each case study is associated with data on its geological background, derived
51 from the wider literature, and including geological age, tectonic setting, prevailing climate conditions,
52 and basin subsidence rates (gathered from total-subsidence curves available in the wider literature; see
53 Cosgrove et al. 2021c).

54 Primary data have been extracted from published accounts, such as sedimentary logs or outcrop
55 panels. Herein, architectural elements are considered in detail, and defined as distinct sedimentary
56 bodies that are the product of deposition in a specific sub-environment. Definitions of architectural-
57 element types mentioned in the text are given in Supplementary Information 3. Architectural elements
58 are classified on interpreted origin (e.g., dune, interdune, sandsheet); their maximum observed
59 thickness is recorded. The proportions of architectural elements in successions, or parts thereof, is
60 considered as fractions of total recorded thicknesses.

61 To enable comparisons between eolian systems developed under different environmental conditions,
62 case studies and data extracted therefrom are grouped according to 1) prevailing climatic conditions
63 (icehouse versus greenhouse), 2) supercontinental setting, 3) the presence or absence of land plants
64 and grasses, and 4) rates of basin subsidence. In addition, data are grouped according to geological
65 age (Proterozoic, Paleozoic, Mesozoic and Cenozoic), to determine the importance of environmental
66 forcings through time.

67 Statistical analysis has been undertaken on element thickness data. Two-tailed t-tests and Independent
68 Group ANOVA have been used to compare mean thicknesses across eolian systems. An α value of
69 0.05 is considered for all statistical analyses.

70 **RESULTS**

71 In the text, for brevity, mean thicknesses are reported; for values of median, standard deviation and
72 number of observations, refer to Table 1. All data shown in the figures are reported in Supplementary
73 Information 4.

74 **Environmental Forcings**

75 Through geological time, the Earth's climate has fluctuated between two end-member climatic
76 conditions: icehouse and greenhouse, respectively defined by the presence or absence of major
77 continental ice-sheets and polar ice (Frakes et al., 1992). Data are grouped according to the prevailing
78 climatic conditions at the time of eolian accumulation (Fig.1A). When all eolian elements are
79 considered, their mean thicknesses are 2.7 m and 4.1 m for icehouse and greenhouse successions,
80 respectively. Greenhouse eolian elements are significantly thicker than their icehouse counterparts
81 ($P < 0.01$; Table 1).

82 Continental masses have undergone cycles of supercontinent assembly and subsequent break-up
83 through geological time (Condie, 2016). Data are grouped according to supercontinental settings (Fig.
84 1B). Mean thicknesses of eolian elements are 1.9 m, 1.5 m, 2.8 m, 7.4 m, and 2.8 m for 1) Proterozoic
85 Rodinia and Pannotia, 2) Gondwana, 3) Pangea, 4) Laurasia and Gondwanaland, and 5) dispersed
86 continental settings, respectively. There is a significant difference amongst groups ($P < 0.01$; Table 1).
87 The thickest eolian elements are associated with the supercontinents Laurasia and Gondwana (175 –
88 65 Ma, following the break-up of Pangea).

89 Rates of basin subsidence are grouped into slow (1-10 m/Myr), moderate (10-100 m/Myr), and rapid
90 (> 100 m/Myr) rates (Fig. 1D). When all eolian elements are considered, mean thicknesses are 2.0 m,
91 3.4 m, and 8.7 m in slowly, moderately, and rapidly subsiding basins, respectively. Mean differences
92 across groups are statistically significant ($P < 0.01$; Table 1).

93 Vascular land plants and grasses evolved at ca. 420 and ca. 66 Ma, respectively (Boyce and Lee,
94 2017). Data are therefore grouped into bins of 2400 – 420 Ma (eolian accumulation prior to the
95 widespread evolution of vascular land plants), 420 – 66 Ma (accumulation in the presence of vascular
96 land plants), and 420 – 0 Ma (accumulation in the presence of vascular land plants and grasses; Fig.
97 1C). When all eolian elements are considered, mean thicknesses are 2.3 m, 4.5 m, and 4.3 m, for
98 eolian systems deposited in ranges of 2400 – 420 Ma, 420 – 66 Ma, 420 – 0 Ma, respectively. A
99 significant difference amongst groups is present ($P < 0.01$; Table 1). Eolian elements developed in the

100 absence of vascular land plants are significantly thinner than those developed under the presence of
101 vascular land plants.

102 **Geological Age**

103 Eolian systems are grouped as deposits of Proterozoic (2400-541 Ma), Paleozoic (451-252 Ma),
104 Mesozoic (252-66 Ma), and Cenozoic (<66 Ma) age (Fig. 2A). When all eolian elements are
105 considered, mean thicknesses are 2.2 m, 2.2 m, 6.7 m, and 2.8 m in these age groups, respectively.

106 There is a significant difference in the mean thicknesses of dune-sets, sandsheets and interdunes (P
107 <0.01), across age groups (Table 1).

108 Ratios of eolian to non-eolian elements as a fraction of the stratigraphy are 61:39, 73:27, 72:28, and
109 79:21 in the Proterozoic, Paleozoic, Mesozoic and Cenozoic, respectively. Dune-sets form 46%, 86%,
110 81% and 89%, sandsheets form 49%, 7%, 4%, and 4%, interdunes form 5%, 7%, 15%, and 7% of the
111 total recorded aeolian stratigraphy, in the Proterozoic, Paleozoic, Mesozoic and Cenozoic,
112 respectively. Dune-sets have mean thicknesses of 1.9 m, 3.0 m, 7.8 m, and 5.8 m, sandsheets have
113 mean thicknesses of 3.6 m, 1.0 m, 3.6 m, and 0.4 m, interdunes have mean thicknesses of 0.8m, 0.7
114 m, 2.5 m, and 0.8 m in the Proterozoic, Paleozoic, Mesozoic, and Cenozoic, respectively. The non-
115 eolian lithology is dominantly marine (52%) and fluvial (39%) in the Proterozoic; fluvial (62%) and
116 alluvial (15%) in the Paleozoic; fluvial (67%) and sabkha (14%) in the Mesozoic; and fluvial (42%)
117 and marine (32%) in the Cenozoic.

118 **Environmental Controls through Geological Time**

119 Environmental controls, for example, the assembly and break-up of supercontinents, or prevailing
120 icehouse and greenhouse conditions, can span only parts of a geological era, or multiple geological
121 eras. As such, for each era, the percentage of recorded architectural elements deposited under given
122 environmental conditions are presented (Fig. 3A).

123 **DISCUSSION**

124 **Climate**

125 Greenhouse eolian elements are significantly thinner than their icehouse counterparts (Table 1; Fig.
126 1A). Under icehouse conditions, eolian systems are subject to episodes of glacial accumulation and
127 interglacial deflation, which are driven by Milankovitch-type cyclicity (Milankovitch, 1941). During
128 glacials, drier conditions are associated with strengthened Trade Winds and depressed water-tables:
129 eolian deposits are therefore more likely to be exposed above the baseline of erosion for extended
130 periods, and are thus prone to deflation and reworking (Kocurek and Havholm, 1993; Cosgrove et al.,
131 2021a). Conversely, under greenhouse conditions high eustatic sea levels and relatively more humid
132 conditions generally promote elevated water tables situated close to the accumulation surface,
133 allowing eolian elements to be rapidly sequestered beneath the erosional baseline and protected from
134 post-depositional reworking (Kocurek et al., 2001). Uniquely in the Mesozoic, eolian accumulation
135 occurred exclusively under greenhouse conditions, which may partly account for the preservation of
136 significantly thicker eolian elements. The roles of humid greenhouse conditions can be inferred by the
137 high percentage of sabkha elements, which is greater than in other eras (Fig. 2B).

138 In the Cenozoic, despite the majority of eolian elements being deposited under icehouse conditions –
139 associated with thinner eolian elements – average dune-set thickness is the second thickest in
140 geological history (Figs. 2A, 3A). Many relatively thick Cenozoic dune-sets are an artefact of
141 preservational biases in that they are not yet truly preserved in a long-term sense as they lie above the
142 level of a long-term erosional baseline: they are accumulated but not yet preserved (*sensu* Kocurek
143 and Havholm, 1993). However, comparisons between Quaternary (<2.6 Ma) and earlier Cenozoic
144 deposits suggest a more complicated relationship: Quaternary deposits are significantly ($P < 0.01$)
145 thinner than their Paleogene (ca. 66-23 Ma) and Neogene (ca. 23-2.6 Ma) counterparts (Table 1). The
146 relative thickness of Cenozoic dune-sets might be due to the evolution of stabilizing grasses at ~66
147 Ma, which limit the capacity for eolian deflation (see below).

148 **Vegetation**

149 Eolian elements deposited in the presence of vascular land plants and grasses are significantly thicker
150 than those that were deposited in their absence (Fig. 1C; Table 1). In the absence of vegetation,
151 substrates lack sediment-binding plant roots; this tends to result in the increased mobility of fluvial
152 channels, which can more easily wander across eolian landscapes and rework eolian sediments
153 (Davies et al., 2011; Santos et al., 2017, 2019; Basilici et al., 2021a). The absence of vascular land
154 plants in the Proterozoic and early Paleozoic (Boyce and Lee, 2017; Fig. 3A) may, in part, account for
155 the preservation of relatively thin eolian dune-sets, and relatively high percentages of sandsheets
156 during these time periods. Sandsheets can represent the erosional remnants of landforms of originally
157 higher relief; their occurrence can represent the reworking of dune bedforms by fluvial processes
158 (Nielsen and Kocurek, 1986). The highest recorded percentage of interdigitating non-eolian elements
159 in Proterozoic successions can be interpreted in these terms (Fig. 2B).

160 The radiation of grasses at 66 Ma has likely further limited the mobility of Cenozoic river systems
161 (Davies-Colley, 1997; Fig. 3). Moreover, grasses play a crucial role in dune construction and
162 stabilization, by disrupting primary airflows in the near-surface layer, decelerating winds and causing
163 the fall-out of airborne sand (Nielsen and Kocurek, 1986; Jackson et al., 2019). After sediment
164 deposition, grasses can effectively trap eolian sediment, inhibiting re-suspension and erosion (Byrne
165 and McCann, 1990; Ruz and Allard, 1994). Grasses can inhibit the deflation of dune-sets, and a
166 record of this can be interpreted in the low percentage of sandsheets in Cenozoic eolian stratigraphies;
167 the stabilizing effects of grasses act to markedly retard eolian winnowing, thereby reducing the supply
168 of sediment suitable for sandsheet accumulation (Nielsen and Kocurek, 1986).

169 **Basin Subsidence and Supercontinental Setting**

170 Long-term eolian preservation requires the generation of accommodation in which deposits can
171 accumulate - most obviously provided by the subsidence of active sedimentary basins (Kocurek and
172 Havholm, 1993). Mesozoic systems developed in basins with significantly higher rates of subsidence
173 (Fig. 2A); they record the highest proportion of stratigraphy accumulated in rapidly subsiding basins
174 (Fig. 3A). Rapid Mesozoic subsidence may correspond with the break-up of Pangea, during which

175 continental rifting led to the formation of Laurasia and Gondwana (Blakey et al., 1988; Condie, 2016).
176 Rapid subsidence enables a faster rate of rise of the level of the accumulation surface, which allows
177 bedforms to climb at steeper angles (Kocurek and Havholm, 1993; George and Berry, 1997; Howell
178 and Mountney, 1997; Paim and Scherer, 2007; Cosgrove et al., 2021c), leading to the preservation of
179 thicker eolian elements.

180 Conversely, the Proterozoic has the highest percentage of eolian elements accumulated in slowly
181 subsiding basins, where eolian elements are thinnest on average (Figs. 2A, 3A). The slow generation
182 of accommodation may have favored the accumulation and preservation of relatively thin genetic
183 eolian units, whereby eolian dune-sets likely climbed at low-angles and accumulated sporadically
184 between long episodes of sediment bypass under conditions of low rates of accommodation
185 generation (e.g. Basilici et al., 2020b; Cosgrove et al., 2021c). Proterozoic systems may be affected by
186 preservational biases, such that the outcropping remains of Proterozoic supercontinents are
187 preferentially preserved in intracratonic basins in ancient, stable continental interiors (Shaw et al.,
188 1991; Aspler and Chiarenzelli, 1997); basins of this type tend to experience slower subsidence rates
189 compared to other settings (Xie and Heller, 2009). However, preserved deposits of Proterozoic eolian
190 systems accumulated in more rapidly subsiding basins are also known (e.g. eolian systems from the
191 rift-sag Espinhaço Basin; Simplicio and Basilici, 2015; Abrantes et al., 2020; Mesquita et al., 2021).

192 **CONCLUSIONS**

193 This study presents the first large-scale quantitative assessment of how environmental forcings have
194 influenced eolian architecture through geological time. Significant differences in eolian architecture
195 are attributed to the interplay of 1) climate, 2) continental configuration, 3) land-plant evolution, and
196 4) basin subsidence (Fig. 3). The independent effect of each of these forcings on the eolian
197 stratigraphic record has been demonstrated statistically. Each of these forcings may span only parts of
198 a geological era, or multiple geological eras, leading to complex interactions between forcing
199 mechanisms throughout Earth history. Results presented here demonstrate how eolian successions

200 record variations in eolian landscapes and sediment preservation mechanisms in response to changes
201 in the Earth's atmosphere, biosphere and geosphere.

202 **ACKNOWLEDGMENTS**

203 We thank the sponsors and partners of FRG-SMRG-ERG for financial support for this research.
204 Claiton Scherer and two anonymous reviewers are thanked for their useful comments.

205 **FIGURE CAPTIONS**

206 1) Thicknesses of eolian and non-eolian architectural elements subdivided by: A) climate (data are
207 grouped into icehouse and greenhouse periods), B) supercontinental setting, C) the presence and type
208 of vegetation, and D) rates of basin subsidence. The legend describing all box and whisker plots is
209 shown in Part C. Outliers are not presented.

210 2) Variations through geological time in: A) thicknesses of eolian and non-eolian architectural
211 elements and rates of basin subsidence (outliers are not presented); B) assemblages of architectural
212 elements.

213 3) A) Percentages of recorded architectural elements deposited under a variety of environmental
214 conditions; B) environmental forcings governing eolian construction, accumulation and preservation
215 through geological time.

216 **TABLE CAPTIONS**

217 1) Results of statistical analyses. Unless otherwise stated, analysis has been completed on all
218 eolian architectural element types.

219 **SUPPLEMENTARY FILES**

220 Supplementary Figure 1) Location map of the 55 ancient eolian case-studies.

221 Supplementary Table 1) List of case-studies and associated source literature.

222 Supplementary Table 2) Definitions of architectural elements and types discussed in the text.

223 Supplementary Table 3) Data used to generate the results presented here.

224 REFERENCES

225 Abrantes, Jr., F.R., Basilici, G., Soares, M.V.T., 2020, Mesoproterozoic erg and sand sheet system:
226 architecture and controlling factors (Galho do Miguel Formation, SE Brazil), *Precambrian Research*,
227 v. 338, 105592. DOI: 10.1016/j.precamres.2019.105592

228 Aspler, L.B. and Chiarenzelli, J.R., 1997, Initiation of 2.45–2.1 Ga intracratonic basin sedimentation of
229 the Hurwitz Group, Keewatin Hinterland, Northwest Territories, Canada, *Precambrian Research*, v. 81,
230 p. 265-297. DOI: 10.1016/S0301-9268(96)00038-1

231 Basilici, G., Mesquita, A.S., Soares, M.V.T., Moutney, N.P. and Colombera, L., 2020, A
232 Mesoproterozoic hybrid dry-wet aeolian system: Galho do Miguel Formation, SE Brazil. *Precambrian*
233 *Research*, v. 359, 106216. DOI: 10.1016/j.precamres.2021.106216

234 Basilici, G., Soares, M.V.T., Moutney, N.P. and Colombera, L., 2020, Microbial influence on the
235 accumulation of Precambrian eolian deposits (Neoproterozoic, Venkatpur Sandstone Formation,
236 Southern India), *Precambrian Research*, v. 347, 105854. DOI:10.1016/j.precamres.2020.105854

237 Blakey, R. C., Peterson, F. and Kocurek, G., 1988, Synthesis of late Paleozoic and Mesozoic eolian
238 deposits of the western interior of the United States, *Sedimentary Geology*, v. 56, p. 3–125. DOI:
239 10.1016/0037-0738(88)90050-4

240 Boyce, K.C. and Lee, J-E., 2017, Plant evolution and climate over geological timescales, *Annual*
241 *Review of Earth and Planetary Sciences*, v. 45, p. 61-87. DOI: 10.1146/annurev-earth-063016-015629

242 Byrne, M.-L. and McCann, S.B., 1989, Stratification models for vegetated coastal dunes in Atlantic
243 Canada, *Sedimentary Geology*, v. 66, p. 165-179. DOI: 10.1016/0037-0738(90)90058-2

244 Clemmensen, L.B., Øxnevad, I.E.I. and de Boer, P.L., 1994, Climatic controls on ancient desert
245 sedimentation: some late Palaeozoic examples from NW Europe and the western interior of the USA.
246 In de Boer, P.L., and Smith, D.G., eds., *Orbital Forcing and Cyclic Sequences*, International Association
247 of Sedimentologists Special Publication, v. 19, p. 439-457. DOI: 10.1002/9781444304039.ch27

248 Condie, K.C., 2016, The supercontinent cycle, *Earth as an Evolving Planetary System*. In K.C. Condie,
249 K.C., eds., *Earth as an Evolving Planetary System (Third Edition)*, Academic Press, p. 201-235. DOI:
250 10.1016/B978-0-12-803689-1.00007-9.

251 Cosgrove, G.I.E., Colombera, L. and Mountney, N.P, 2021a, Quantitative analysis of the sedimentary
252 architecture of eolian successions developed under icehouse and greenhouse climatic conditions.
253 *Geological Society of America Bulletin*. DOI: 10.1130/B35918.1

254 Cosgrove, G.I.E., Colombera, L. and Mountney, N.P, 2021b, A database of Eolian Sedimentary
255 Architecture for the characterization of modern and ancient sedimentary systems, *Marine and Petroleum*
256 *Geology*, v. 127, 104983. DOI: 10.1016/j.marpetgeo.2021.104983.

257 Cosgrove, G.I.E., Colombera, L. and Mountney, N.P, 2021c, The role of subsidence and
258 accommodation generation in controlling the nature of the aeolian stratigraphic record, *Journal of the*
259 *Geological Society*. DOI: 10.1144/jgs2021-042

260 Davies, N. S., Gibling, M. R. and Rygel, M. C., 2011, Alluvial facies during the Palaeozoic greening
261 of the land: case studies, conceptual models and modern analogues, *Sedimentology*, p. 58, v. 220–258.
262 DOI: 10.1111/j.1365-3091.2010.01215.x

263 Davies-Colley, R.J., 1997, Stream channels are narrower in pasture than in forest, *New Zealand Journal*
264 *of Marine and Freshwater Research*, v. 31, p. 599-608. DOI: 10.1080/00288330.1997.9516792

265 Frakes, L.A., Francis, J.E., and Syktus, J.I., 1992, *Climate modes of the Phanerozoic*, New York:
266 Cambridge University Press, pp. 274. DOI: 10.1017/CBO9780511628948

267 George, G.T., and Berry, J.K., 1997, Permian (Upper Rotliegend) synsedimentary tectonics, basin
268 development and palaeogeography of the southern North Sea. In Ziegler, P., Turner, P., and Daines,
269 S.R., eds., Petroleum geology of the southern North Sea, Geological Society of London Special
270 Publication, v. 123, p. 31–61. DOI: 10.1144/GSL.SP.1997.123.01.04

271 Gibling, M. and Davies, N., 2012, Palaeozoic landscapes shaped by plant evolution. *Nature Geoscience*,
272 v. 5, p. 99–10. DOI: 10.1038/ngeo1376

273 Howell, J.A. and Mountney, N.P., 1997, Climatic cyclicity and accommodation space in arid and semi-
274 arid depositional systems: an example from the Rotliegende Group of the southern North Sea. In North,
275 C.P., and Prosser, J.D., eds., *Petroleum Geology of the Southern North Sea: Future Potential*, Geological
276 Society of London Special Publication, v. 123, p. 199-218. DOI: 10.1144/GSL.SP.1997.123.01.05

277 Jackson, D.W.T., Costas, S., González-Villanueva, R. and Cooper, A., 2019, A global ‘greening’ of
278 coastal dunes: An integrated consequence of climate change?, *Global and Planetary Change*, v. 182,
279 103026. DOI: 10.1016/j.gloplacha.2019.103026.

280 Kocurek, G. and Dott, R.H., 1981, Distinctions and uses of stratification types in the interpretation of
281 eolian sand, *Journal of Sedimentary Petrology*, v. 51, p. 579-595. DOI: 10.1306/212F7CE3-2B24-
282 11D7-8648000102C1865D

283 Kocurek, G. and Havholm, K.G., 1993, Eolian sequence stratigraphy-a conceptual framework. In
284 Weimer, P., and Posamentier, H., eds., *Siliciclastic Sequence Stratigraphy*, American Association of
285 Petroleum Geologists Memoir, v. 58, p. 393-409. DOI: 10.1306/M58581C16.

286 Kocurek, G., Robinson, N.I. and Sharp, J.M.J., 2001, The response of the water table in coastal aeolian
287 systems to changes in sea level, *Sedimentary Geology*, v. 139, p. 1-13. DOI: 10.1016/S0037-
288 0738(00)00137-8

289 Mesquita, A.F., Basilici, G., Soares, M.V.T. and Garcia, R.G.V., 2021, Morphology, accumulation and
290 preservation of draa systems in a Precambrian erg (Galho do Miguel Formation, SE Brazil),
291 *Sedimentary Geology*, v. 412, 105807. DOI: 10.1016/j.sedgeo.2020.105807

292 Milankovitch, M., 1941, *Kanon der Erdbestrahlung und seine Anwendung auf das Eiszeiten-problem*,
293 Royal Serbian Academy, Belgrade

294 Mountney, N.P. and Jagger, A., 2004, Stratigraphic evolution of an eolian erg margin system: the
295 Permian Cedar Mesa Sandstone, SE Utah, USA, *Sedimentology*, v. 51, p. 713-743. DOI:
296 10.1111/j.1365-3091.2004.00646.x

297 Nielson, J. and Kocurek, G., 1986, Climbing zibars of the Algodones, *Sedimentary Geology*, v. 48, p.
298 1-15. DOI: 10.1016/0037-0738(86)90078-3

299 Paim, P.S.G. and Scherer, C.M.S., 2007, High-resolution stratigraphy and depositional model of wind-
300 and water-laid deposits in the Ordovician Guaritas Rift (southernmost Brazil), *Sedimentary Geology*,
301 v. 202, p. 776-795. DOI: 10.1016/j.sedgeo.2007.09.003

302 Rodríguez-López, J.P., Clemmensen, L.B., Lancaster, N., Mountney, N.P. and Veiga, G.D., 2014,
303 Archean to Recent eolian sand systems and their sedimentary record: Current understanding and future
304 prospects, *Sedimentology*, v. 61, p. 1487-1534. DOI: 10.1111/sed.12123

305 Ruz, M.-H. and Allard, M., 1994, Coastal dune development in cold-climate environments, *Physical*
306 *Geography*, v. 15, p. 372–380. DOI: 10.1080/02723646.1994.10642523

307 Santos, M.G.M., Mountney, N.P. and Peakall, J., 2017, Tectonic and environmental controls on
308 Palaeozoic fluvial environments: reassessing the impacts of early land plants on sedimentation, *Journal*
309 *of the Geological Society*, v. 16, p. 393–404. DOI: 10.1144/jgs2016-063

310 Santos, M.J.M., Hartley, A.J., Mountney, N.P., Peakall, J., Owen, A., Merino, E.R., Assine, M.L., 2019,
311 Meandering rivers in modern desert basins: Implications for channel planform controls and
312 prevegetation rivers, *Sedimentary Geology*, v. 385, p. 1-14. DOI: 10.1016/j.sedgeo.2019.03.011.

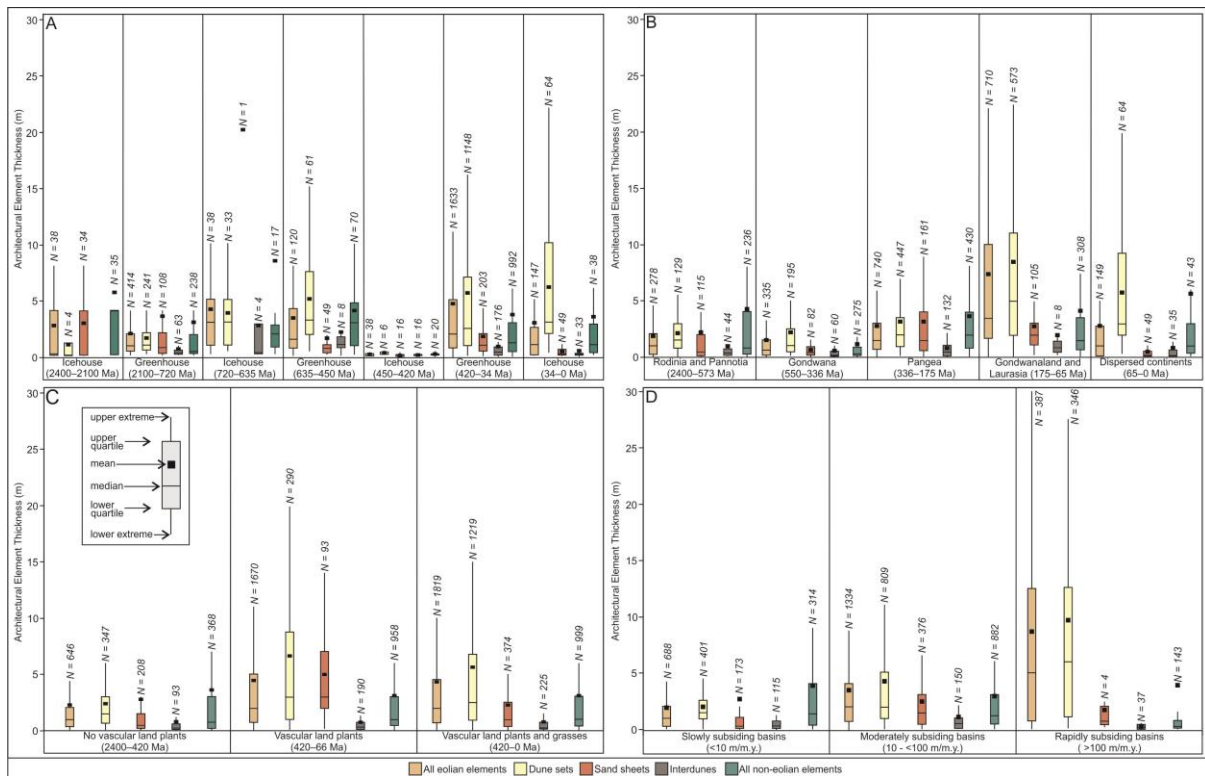
313 Scotese, C.R. and Barrett, S.F., 1990, Gondwana's movement over the South Pole during the Palaeozoic:
 314 evidence from lithological indicators of climate, Geological Society of London Memoirs, v. 12, p. 75-
 315 85. DOI: 10.1144/GSL.MEM.1990.012.01.06

316 Shaw, R.D., Etheridge, M.A. and Lambeck, K., 1991, Development of the Late Proterozoic to Mid-
 317 Paleozoic, intracratonic Amadeus Basin in central Australia: A key to understanding tectonic forces in
 318 plate interiors, Tectonics, v. 10, p. 688-721. DOI: 10.1029/90TC02417

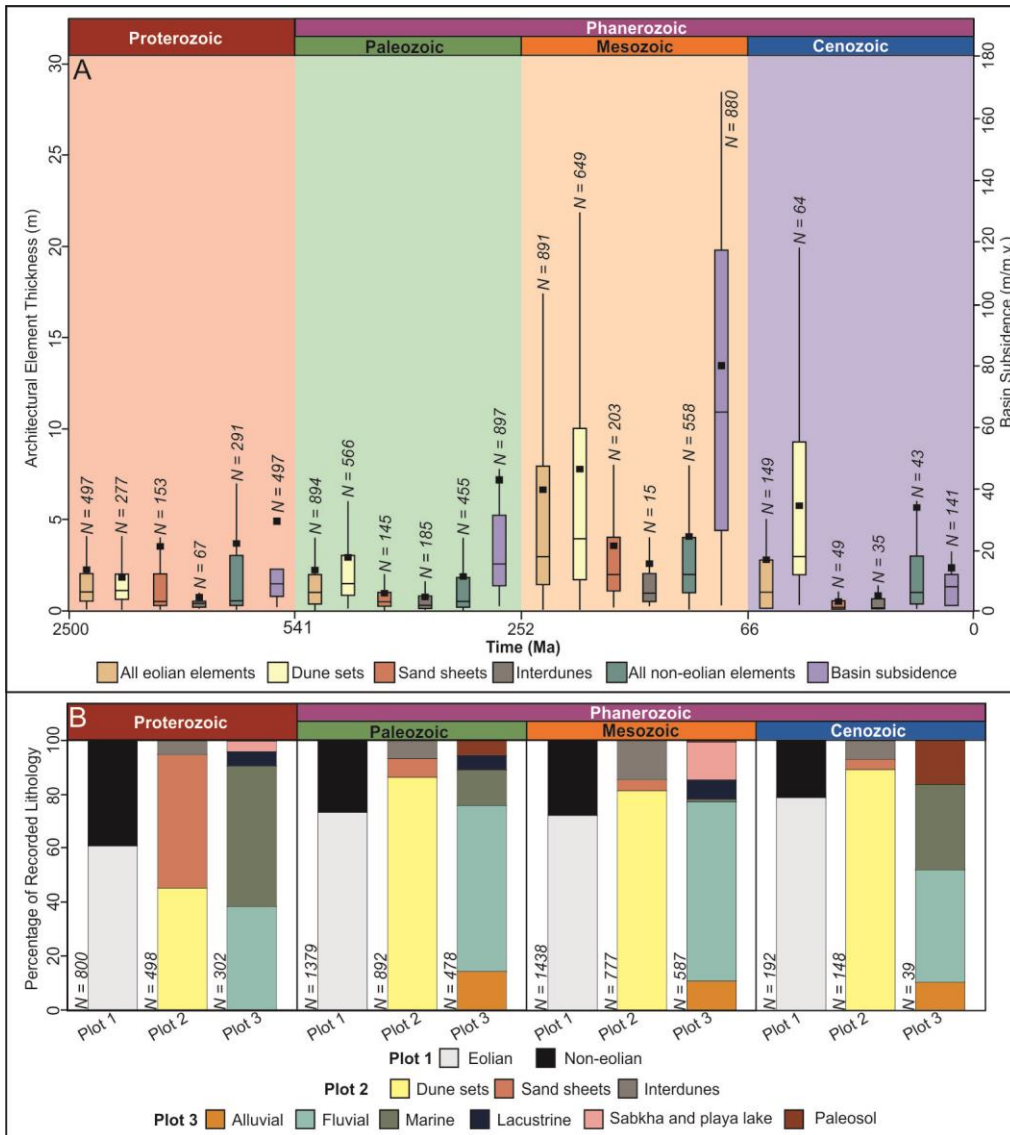
319 Simplicio, F. and Basili, G., 2015, Unusual thick eolian sand sheet sedimentary succession:
 320 Paleoproterozoic Bandeirinha Formation, Minas Gerais, Brazilian Journal of Geology, v. 45, p. 3-11.
 321 DOI: 10.1590/2317-4889201530133

322 Xie, X. and Heller, P.L., 2009, Plate tectonics and subsidence history, Geological Society of America
 323 Bulletin, v. 121, p. 55-64. DOI:10.1130/B26398.1

324 **Figure 1**



325
 326
 327



329

